Ligand Binding by Antibody IgE Lb4: Assessment of Binding Site Preferences Using Microcalorimetry, Docking, and Free Energy Simulations

Christoph A. Sotriffer,* Wolfgang Flader,* Alan Cooper,# Bernd M. Rode,* D. Scott Linthicum,§ Klaus R. Liedl,* and Janos M. Varga*

*Institute of General, Inorganic and Theoretical Chemistry, University of Innsbruck, A-6020 Innsbruck, Austria; #Department of Chemistry, Glasgow University, Glasgow G12 8QQ, Scotland; and §Department of Pathobiology, Texas A & M University, College Station, Texas 77843-4467 USA

ABSTRACT Antibody IgE Lb4 interacts favorably with a large number of different compounds. To improve the current understanding of the structural basis of this vast cross-reactivity, the binding of three dinitrophenyl (DNP) amino acids (DNP-alanine, DNP-glycine, and DNP-serine) is investigated in detail by means of docking and molecular dynamics free energy simulations. Experimental binding energies obtained by isothermal titration microcalorimetry are used to judge the results of the computational studies. For all three ligands, the docking procedure proposes two plausible subsites within the binding region formed by the antibody CDR loops. By subsequent molecular dynamics simulations and calculations of relative free energies of binding, one of these subsites, a tyrosine-surrounded pocket, is revealed as the preferred point of complexation. For this subsite, results consistent with experimental observations are obtained; DNP-glycine is found to bind better than DNP-serine, and this, in turn, is found to bind better than DNP-alanine. The suggested binding mode makes it possible to explain both the moderate binding affinity and the differences in binding energy among the three ligands.

INTRODUCTION

Antibodies are generally considered to be highly specific defense agents of the immune system against invading antigens. In contrast to this general notion of specificity, over the last several years a growing number of cross-reactive antibodies has become known, which bind not only the immunizing antigen, but also other ligands with similar affinity (e.g., Richards et al., 1975; Czaja et al., 1976; Varga et al., 1991a,b; Arevalo et al., 1993; Chitarra et al., 1993; Carlin et al., 1994; Roggenbuck et al., 1994; Shreder et al., 1996; Lamminmäki et al., 1997). Structurally, however, only a small subset of these antibodies and their complexes has been characterized so far, and consequently it was stated that the structural basis for antibody polyreactivity is not yet clear (Padlan, 1994).

Antibody IgE-Lb4 is an example of a highly cross-reactive antibody. It belongs to a class of anti-trinitrophenyl antibodies and was recognized to be heteroclitic, i.e., ligands different from the immunizing hapten are bound with higher affinity (Furusawa and Ovary, 1988). Subsequently, Lb4 was studied to characterize its binding properties in more detail. Screening assays (Varga et al., 1991a) with over 2000 different compounds revealed several classes of molecules bound by Lb4, although in many cases no obvious structural similarities could be observed (Winger et al., 1996). The variable region genes for IgE Lb4 were cloned and sequenced (Kofler et al., 1992). The resulting information was used to obtain the structure of the variable region fragment (Fv) by homology modeling (Droupadi et al., 1994). Comparative docking studies were then performed to obtain first indications of how the binding of different ligands could be understood in structural terms (Sotriffer et al., 1996; Winger et al., 1996).

To further elucidate the structural and energetic basis of the cross-reactive binding properties of antibody Lb4, this work is focused on the investigation of the complexes formed with three dinitrophenyl (DNP) amino acids (DNP-alanine, DNP-glycine, and DNP-serine, as shown in Fig. 1).

To derive structural insights, a combination of computational approaches is used, including new docking searches with refined procedures and free energy calculations using molecular dynamics simulations. An experimental thermodynamic analysis of the complexes is carried out by means of isothermal titration microcalorimetry. The accurate experimental binding data obtained by this method allow us to validate the results of the calculations.

The compounds investigated here were selected from the pool of known Lb4-ligands based on requirements of the free energy simulation method. Therefore three DNP-amino acids were chosen that show only slight structural differences among themselves. This makes the simulations more feasible and helps to avoid more severe sampling and convergence problems. Furthermore, the nature of the chosen ligands allows us to calculate the relative free energy difference for all three ligand pairs in turn and thus to carry out an internal consistency check of the results. The disadvantage of the structural similarity of the ligands is that differences in binding free energy could turn out to be relatively small. However, as shown in an excellent study by Pearl-

Received for publication 7 October 1998 and in final form 18 March 1999.

Address reprint requests to Dr. Klaus R. Liedl, Department of Theoretical Chemistry, Institute of General, Inorganic, and Theoretical Chemistry, University of Innsbruck, Innrain 52a, A-6020 Innsbruck, Austria. Tel.: 43-512-507-5164; Fax: 43-512-507-5144; E-mail: klaus.liedl@uibk.ac.at.

0006-3495/99/06/2966/12 $2.00

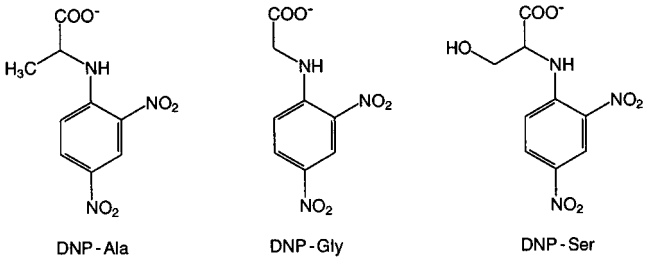

FIGURE 1 Structures of the investigated ligands.

man and Connelly (1995), who analyzed the effect of a tyrosine-to-phenylalanine mutation associated with a 0.60 kcal/mol change in ligand affinity, minor free energy differences can also be successfully analyzed if the structural prerequisites are met and sensible simulation protocols are applied.

MATERIALS AND METHODS

Microcalorimetry

Isothermal titration calorimetry (ITC) experiments to measure the binding of DNP-amino acids (DNP-Ala, DNP-Gly, DNP-Ser) to Lb4 were conducted at 25°C, using a Microcal OMEGA titration microcalorimeter and following standard instrumental procedures (Wiseman et al., 1989; Cooper and Johnson, 1994; Fisher and Singh, 1995), with a 250-μl injection syringe and 400 rpm stirring. The monoclonal antibody Lb4 was purified to homogeneity by affinity chromatography as described (Droupadi et al., 1994), subsequently dialyzed overnight at 4°C in buffer (50 mM sodium phosphate, 0.1 M NaCl, 0.01% sodium azide, pH 7.2), and gently degassed immediately before use. DNP-ligands were dissolved in the same dialysis buffer. Protein concentrations in the ITC cell were determined from UV absorbance measurements at 280 nm, using $\epsilon_{280} = 239{,}000$ as the molar extinction coefficient. A typical binding experiment involved 25 $\times$ 10-μl injections of ligand solution (typically around 0.4 mM concentration) into the ITC cell ($\sim$1.3 ml active volume) containing protein ($\sim$10 μM). Control experiments were performed under identical conditions by injection of the ligand into buffer alone (to correct for heats of ligand dilution) and injection of buffer into the protein mix (to correct for heats of dilution of the protein). Integrated heat effects, after correction for heats of dilution, were analyzed by nonlinear regression in terms of a simple single-site binding model, using the standard Microcal ORIGIN software package. For each thermal titration curve, this yields estimates of the apparent number of binding sites (N) on the protein, the binding constant (K [M^{-1}]; also expressed as the reciprocal dissociation constant, K_{diss} [μM]), and the enthalpy of binding (ΔH [kcal/mol]). Other thermodynamic quantities were calculated using standard expressions: $\Delta G^\circ = -RT \ln K = \Delta H^\circ - T\Delta S^\circ$.

Docking

The Fv structure of Lb4 obtained by means of homology modeling by Droupadi et al. (1994) was used for all computational studies. For antibodies, this method of structure prediction is sufficiently reliable, given the special characteristics of this class of proteins (stability of the immunoglobulin-fold; limited number of canonical structures for the hypervariable loops; Chothia and Lesk, 1987) and the availability of a large number of experimental structures (Padlan, 1996). Examination of the Lb4 sequence revealed that key residues known to create specific canonical conformations of the complementarity determining region (CDR) loops are present in the required positions. Furthermore, no insertions or deletions were needed in the "parent" loop structures selected as templates for the CDR loops of Lb4. These two facts not only facilitated the modeling process, but also increased the reliability of the Lb4 structure obtained.

Docking was performed with version 2.4 of the program AutoDock (Morris et al., 1996; Goodsell and Olson, 1990). For consistency with subsequent molecular dynamics (MD) simulations, the force-field parameters were taken from the new AMBER force field (Cornell et al., 1995). This required the assignment of the corresponding charges to Lb4 as well as charge calculations for the ligands by fitting to the HF/6–31G* electrostatic potential. The necessary ab initio calculations were performed with GAUSSIAN94 (Frisch et al., 1995), the restrained electrostatic potential fit with the RESP program (Bayly et al., 1993; Cornell et al., 1993). Following the philosophy of the new AMBER force field, no special hydrogen bonding term was applied. For evaluation of the Coulomb interactions, a sigmoidal distance-dependent dielectric function was used (Mehler and Solmajer, 1991). The affinity grids were centered on the CDRs, with dimensions of 45 Å $\times$ 36 Å $\times$ 43 Å and a grid spacing of 0.5 Å. The simulated annealing search process was started at a temperature corresponding to $RT = 1200$ cal/mol, which was reduced by a factor of 0.90 after each cycle. A cycle consisted of a maximum of 30,000 accepted or rejected steps, where a step corresponds to a random change in translational, rotational, and torsional degrees of freedom of the ligand. One hundred such cycles were performed per docking run, and for each ligand 100 independent docking runs were carried out.

In numerous studies AutoDock has been shown to successfully reproduce experimental protein-ligand interaction geometries (Goodsell and Olson, 1990; Goodsell et al., 1993; Friedman et al., 1994; Morris et al., 1996; Coutinho et al., 1997). The parameters used here were tested on an antibody-hapten complex (AN02; Brünger et al., 1991) used in a previous study (Sotriffer et al., 1996). The success rate obtained with the new protocol was higher, with 54 of 100 runs reproducing the x-ray structure and being correctly ranked with top docking energies. Again, only one alternative result orientation was found in the rest of the runs and ranked with considerably worse energy. Further studies on experimental antibody-hapten complexes using this docking method are presented elsewhere (Sotriffer et al., 1999).

Free energy simulations

Differences in free energy of binding to Lb4 were calculated for DNP-Ala relative to DNP-Gly, DNP-Ser relative to DNP-Ala, and DNP-Ser relative to DNP-Gly. This allowed us to establish a closed thermodynamic cycle (DNP-Ser $\rightarrow$ DNP-Ala $\rightarrow$ DNP-Gly $\rightarrow$ DNP-Ser) as an internal consistency check (Mark et al., 1994; Essex et al., 1997), as the free energy change in a closed cycle should obviously be 0, irrespective of the methodology used for its evaluation. Calculations were performed for two different binding orientations suggested by the docking procedure.

Relative free energies of binding were obtained by the technique of thermodynamic integration (TI) along nonphysical pathways, where ligand 1 is mutated into ligand 2, both in aqueous solution and complexed to the antibody in solution. The method is described and reviewed in several articles (Beveridge and DiCapua, 1989; Reynolds et al., 1992; Straatsma and McCammon, 1992; Kollman, 1993; Pearlman, 1994; Pearlman and Connelly, 1995; Straatsma, 1996; Helms and Wade, 1997). A thermody-

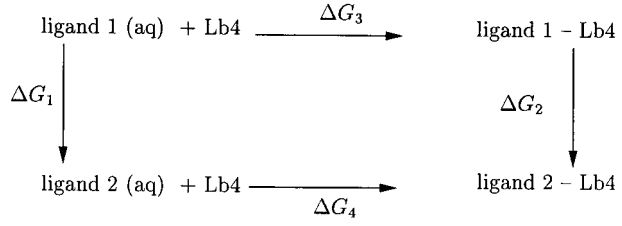

FIGURE 2 Thermodynamic cycle for the evaluation of relative free energies of binding.

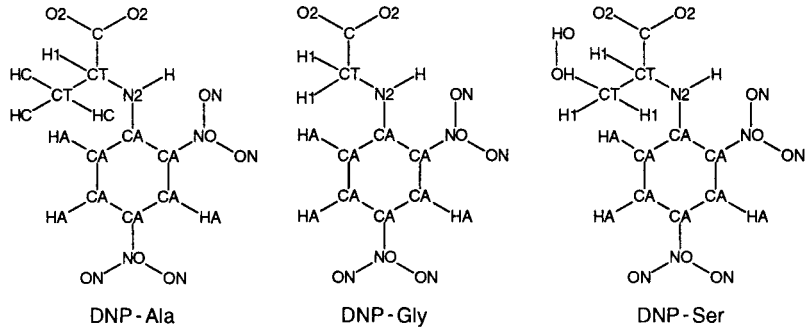

FIGURE 3 Atom types assigned to the ligand atoms.

namic cycle as shown in Fig. 2 was used to establish the relationships between the molecular states under consideration.

The horizontal arrows in Fig. 2 indicate the process of binding between the antibody and the ligand, with the experimentally accessible binding free energies ΔG_3 and ΔG_4. The vertical directions represent the "alchemical process" (Straatsma and McCammon, 1992) corresponding to the "mutation" of the ligand, both in solution (ΔG_1) and complexed by the antibody (ΔG_2). These "mutational pathways" are computationally more easily accessible than the real binding processes given by the horizontal arrows. Through the thermodynamic cycle, however, experimental and theoretical binding energies are directly comparable: because free energy is a state function, $\Delta G_2 - \Delta G_1$ is equal to $\Delta G_4 - \Delta G_3$, and thus the relative free energy of binding $\Delta\Delta G$ can be obtained by experiment as well as by simulation.

To calculate the free energy difference ΔG between two states A and B by thermodynamic integration, the potential functions $V_A(r^N)$ and $V_B(r^N)$ corresponding to states A and B and depending on the coordinates r^N of all atoms in the system, are connected by a so-called coupling parameter λ. The potential function changes from V_A to V_B as λ is varied from 0 to 1:

$$V(\lambda, r^N) = (1 - \lambda)V_A(r^N) + \lambda V_B(r^N).$$

ΔG is then obtained as

$$\Delta G = \int_0^1 \left\langle \frac{\partial V(\lambda, r^N)}{\partial \lambda} \right\rangle_\lambda d\lambda$$

where the angle brackets $\langle\ \rangle$ represent an ensemble average at a given λ. The integral is calculated by evaluating the integrand at a series of discrete λ values ("windows") and applying the trapezoidal method as a numerical integration algorithm.

All simulations and free energy calculations were carried out with the AMBER4.1 series of programs (Pearlman et al., 1995a,b), using the new AMBER force field (Cornell et al., 1995). Six starting configurations had to be prepared: DNP-Ala and DNP-Ser uncomplexed in solution, and DNP-Ala and DNP-Ser complexed to Lb4, each in two different positions. DNP-Ser was used as starting point for the mutations to both DNP-Ala and DNP-Gly, whereas DNP-Ala served only as the starting point for mutations to DNP-Gly. By this setup no definition of dummy atoms in the starting systems was required. The atom types assigned to the ligand atoms are shown in Fig. 3. Additional force-field parameters required for structural units that are not covered by the standard AMBER force field are listed in Table 1. They were derived in comparison with existing parameters, experimental data, and results from ab initio calculations.

The free (unbound) ligands were solvated in a rectangular box of TIP3P water molecules (Jorgensen et al., 1983) with a minimum solute-wall distance of 10 Å. This resulted in a box size of 30 Å × 26 Å × 24 Å and ~510 water molecules within the box. In a first step the systems were energy minimized, to optimize the distribution of the water molecules around the solute. Subsequently, MD simulations were started to equilibrate the systems for the following free energy calculations. After 10 ps of initial gradual heatup to a temperature of 300 K, a further 40 ps was simulated under NPT conditions (300 K and 1 atm) with full periodic boundary conditions. The temperature was kept constant by coupling to a heat bath through the Berendsen algorithm (Berendsen et al., 1984). Pressure was adjusted by isotropic position scaling. All covalent bonds were constrained by the SHAKE algorithm (Ryckaert et al., 1977), and a time step of 2 fs was used. A residue-based cutoff of 8 Å was applied to the noncovalent interactions; the pair list was updated every 10 time steps (0.02 ps).

The complexes were set up for simulation in a similar way. The antibodies with bound ligand where placed in TIP3P water boxes, while maintaining a minimum solute-wall distance of 8 Å. This led to a box size of 68 Å × 65 Å × 56 Å, with ~6100 water molecules and a total of 22,000 atoms. After initial energy minimization and subsequent start of MD simulations with heatup to 300 K in 10 ps, the systems were equilibrated for 90 ps, using the same simulation parameters as given above (for the simulation of the ligands in solution).

The free energy calculations were started with the systems resulting from the equilibration, using the same simulation parameters. The mutations were carried out by the single topology technique, which requires the definition of dummy atoms when the initial and final molecules have different numbers of atoms. The dummy atoms have van der Waals parameters equal to zero and carry no charge (i.e., no interaction with the environment), and bond, angle, and torsional parameters are kept as in the

TABLE 1 Additional force-field parameters for the DNP-ligands

Bonds	K_b (kcal mol^{-1} Å^{-2})		r_0 (Å)
CA—NO	337.0		1.468
NO—ON	656.0		1.217
Angles	K_Θ (kcal mol^{-1} rad^{-2})		Θ_0 (deg)
C—CT—N2	63.0		110.1
CA—CA—NO	70.0		120.0
CA—CA—N2	70.0		120.0
CA—NO—ON	70.0		117.0
ON—NO—ON	80.0		126.0
Dihedrals	K_Φ (kcal mol^{-1})	Phase (deg)	Periodicity
CA—CA—NO—ON	9.6	180.0	2
Improper Dihedrals	K_Φ (kcal mol^{-1})	Phase (deg)	Periodicity
CA—CA—CA—NO	1.1	180.0	2
CA—CA—CA—N2	1.1	180.0	2
CA—ON—NO—ON	10.5	180.0	2
van der Waals Parameters	ϵ (kcal mol^{-1})	R^* (Å)	
ON	0.2100	1.6612	
NO	0.1700	1.8240	

nondummy state. The free energies were calculated, including all intraperturbed group contributions and applying the PMF corrections for contributions arising from bond length changes (Pearlman and Kollman, 1991; van Gunsteren and Mark, 1992; Pearlman and Connelly, 1995). Thermodynamic integration was performed over 21 windows (λ spacing 0.05) with varying times of equilibration and data collection. For the free ligands in solution, simulations were carried out with 2, 4, 6, and 10 ps for each equilibration (eq) and data collection (dc) per window, resulting in total simulation times of 84, 168, 252, and 420 ps, respectively. The complexes were all simulated with 4 ps of equilibration and data collection, respectively, for each window (168 ps total simulation time). For one complex example (the mutation of DNP-Ala to DNP-Gly), a shorter and a longer simulation were run as well (eq/dc/total of 2/2/84 and 10/10/420 ps) to check the convergence behavior.

To avoid numerical instabilities, the mutations from DNP-Ser to DNP-Gly were done with electrostatic decoupling, which implies that two separate simulations have to be carried out. In the case of disappearing atoms, the first simulation is used for the electrostatic perturbation, and the second serves to change the van der Waals parameters. This order is reversed when the mutation is performed in the opposite direction, i.e., when atoms are generated. To avoid problems during particle deletion, there are other approaches, such as the use of a soft-core potential (Beutler et al., 1994) or separation-shifted potential scaling (Zacharias et al., 1994). However, the two methods are not yet implemented in the standard AMBER program, although the former variant has already been used successfully in combination with AMBER in a recent study by Simmerling et al. (1998).

All simulations were done in the forward as well as the backward direction. After each forward simulation, 20 ps of intrarun equilibration was done on the $\lambda = 0$ state before the mutation was started back toward the $\lambda = 1$ state.

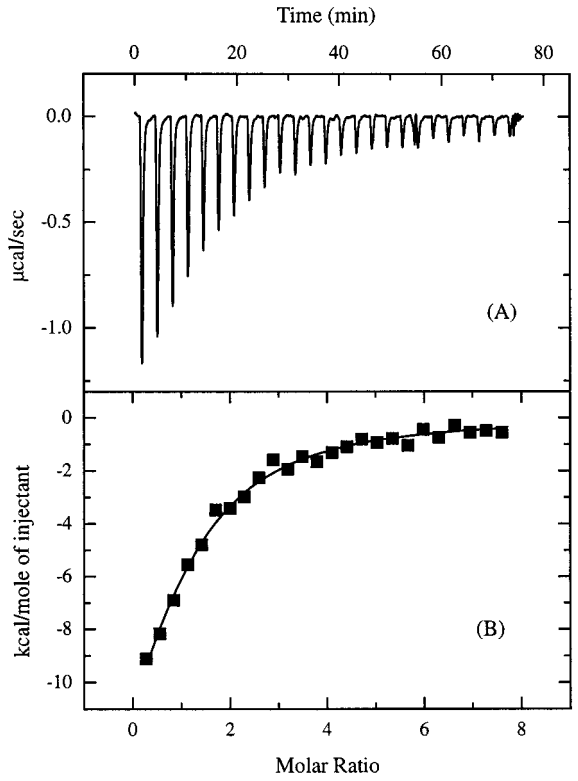

FIGURE 4 Example of calorimetric data for binding of a DNP-ligand to monoclonal antibody. (*A*) Raw ITC data for 25 × 10-μl injections of DNP-Ala (0.39 mM) into Lb4 solution (10 μM) at 25°C, pH 7.2. (*B*) Integrated heats from above, with the theoretical curve (*solid line*) corresponding to 1:1 complexation with parameters given in Table 2, derived by nonlinear regression as described in the text.

RESULTS AND DISCUSSION

Experimental binding energies

Microcalorimetric titration experiments involving the addition of DNP-ligands to Lb4 in solution gave exothermic heat pulses consistent with simple noncovalent binding of ligand to identical antibody sites. Typical data are shown in Fig. 4, and the thermodynamic data derived from these experiments are summarized in Table 2.

Dissociation constants (K_{diss}) are in the 5–15 μM range, corresponding to standard free energies of binding ($\Delta G°$) between −7.3 and −6.6 kcal/mol. Variations in binding enthalpies ($\Delta H°$) are somewhat larger between different ligands, but are mainly offset by compensating changes in entropy of binding ($\Delta S°$). Comparison with an extensive list of association constants of monoclonal antibodies for haptens (Chappey et al., 1994) shows that the binding data obtained here are within the range of what is generally observed but also suggests that the analyzed ligands are bound with comparatively moderate affinity.

As far as the relative free energies of binding are concerned, the binding strength increases in going from DNP-Ala over DNP-Ser to DNP-Gly: DNP-Gly binds 0.5 kcal/mol better than DNP-Ser and 0.7 kcal/mol better than DNP-Ala. Regarding the enthalpic and entropic contributions, the same range of magnitude is observed for DNP-Gly and DNP-Ser, whereas the binding of DNP-Ala is characterized by a somewhat larger enthalpic term and a greater loss in entropy. This may reflect the fact that in contrast to the polar Ser side chain, the methyl group of DNP-Ala is not interacting with water through hydrogen bonds. Consequently, the desolvation enthalpy is smaller and the resulting gain in enthalpy upon binding is larger. Furthermore, the loss in conformational flexibility is higher, leading to a more negative change in entropy.

Docking

The primary objective of docking DNP-Ala, DNP-Gly, and DNP-Ser to Lb4 has been to obtain suggestions about probable binding positions in the most suitable way for subsequent free energy calculations by MD simulations. To accomplish this task, it is preferable to use the same force-field parameters for the docking procedure as for the

TABLE 2 Experimental thermodynamic data for DNP-ligand binding to Lb4, determined by isothermal titration microcalorimetry at 25°C, pH 7.2

	DNP-Ala	DNP-Gly	DNP-Ser
K_{diss} (μM)	14.7 (±2.4)	4.7 (±0.5)	10.6 (±1.0)
$\Delta H°$ (kcal/mol)	−24.4 (±1.5)	−19.3 (±1.3)	−19.4 (±1.8)
$\Delta S°$ (cal/mol K)	−59.6 (±5.4)	−40.4 (±4.5)	−42.2 (±6.4)
$\Delta G°$ (kcal/mol)	−6.6 (±0.1)	−7.3 (±0.1)	−6.8 (±0.1)

simulations, to avoid discrepancies that could lead to artifacts and instabilities during optimization and equilibration. In addition, the search of the configuration space should be carried out as exhaustively as possible to localize all binding alternatives and to analyze in detail whether all ligands can bind in similar positions. The similarity is important for the applicability of standard free energy perturbation techniques, in which small perturbations and close resemblance of the binding positions are advantageous. A former docking study on Lb4 (Sotriffer et al., 1996) had already revealed binding possibilities for the three DNP-ligands. However, these were obtained with different force-field parameters and searches that were less extensive by an order of magnitude, because a large number of compounds had to be covered. Consequently, DNP-Ala, DNP-Gly, and DNP-Ser have now been redocked to Lb4 as described in Materials and Methods, using considerably larger grids and increasing the number of independent runs by a factor of 10.

The docking results obtained in this way are summarized in Table 3. The 100 runs for each ligand gave 25 (DNP-Ala), 33 (DNP-Gly), and 30 (DNP-Ser) different results (i.e., positions differing by more than 1 Å root mean square deviation (rmsd)). This is a less well-defined result than observed for the AN02 test case mentioned above. It has to be kept in mind, however, that the topology of the binding site as well as the nature of the ligands are very different for AN02 and Lb4: AN02 has a deep and narrow binding cleft flanked by two tryptophans, and the AN02 DNP-ligand carries two large, bulky substituents. In contrast, DNP-Ala, DNP-Gly, and DNP-Ser are considerably smaller, and the surface of Lb4 shows larger pockets that appear to be less discriminating. As a consequence, obtaining sharply distributed docking results is more difficult for Lb4, and the primary output needs some further analysis.

Upon visual inspection, the Lb4 results for the three DNP-amino acids could be roughly classified into three groups: a set of results located in a tyrosine-formed pocket (which will be called subsite 1 (S1)), another set accommodated in the cleft already known from the previous docking study (which will be called subsite 2 (S2)), and finally, a heterogeneous group of results found at various locations outside the CDRs and in positions at the top of the surface, where they do not enter any cleft and appear to be bound rather loosely.

The two binding pockets are close neighbors within the CDR region of Lb4, but they are separated by a short segment of the CDR H3 loop, from Trp H95 to Ile H98 (H and L denote heavy and light chain, respectively; residues are numbered according to the system of Kabat et al. (1991)). Subsite 1 is primarily formed by CDR H3. Three tyrosine side chains (Tyr H32, Tyr H102, and Tyr L49) mark the spatial limits of this subsite. Together with these tyrosines, Arg H94, Trp H95, Gly H96, Ile H98, and Lys L50 are among the most important contact residues. For subsite 2, CDR H3 forms the border with Trp H95 and Leu H97 as primary contact residues. Residues from CDR L1 (His L27D, Tyr L32) and CDR L3 (Gly L91, Ser L92, Val L94), as well as Tyr H50 from CDR L2 are important interaction partners as well. Figs. 5 and 6 give an impression of the architecture of the subsites (both figures were prepared using MOLSCRIPT; Kraulis, 1991).

TABLE 3 Overview of docking results

	N_{tot}	N_{diff}	E (kcal/mol)	dS1 (Å)	dS2 (Å)
DNP-Ala					
Total	100	25	−28.36 to −19.25	—	—
Results in S1	20	3	−25.58	5.1	13.0
Results in S2	7	4	−23.83	11.3	3.7
Other results	73	18	−25.97	16.4	18.6
DNP-Gly					
Total	100	33	−30.37 to −21.21	—	—
Results in S1	7	3	−27.61	3.8	12.0
Results in S2	13	5	−23.13	11.1	3.2
Other results	80	25	−24.98	16.4	18.2
DNP-Ser					
Total	100	30	−25.66 to −17.90	—	—
Results in S1	15	3	−23.54	5.1	12.9
Results in S2	20	5	−20.41	11.7	4.2
Other results	65	22	−22.49	17.3	20.1

N_{tot} is the total number of results; N_{diff} is the number of results differing by more than 1 Å rmsd; E is the docking energy. In the Total line the energy range of all results is given, whereas the other lines contain the average energy of the respective results. S1 and S2 are the two subsites, and dS1 and dS2 are the distances from the ligand center to the subsite center. The subsite centers are defined as the geometrical centers of the contact residues given in Table 4. All averages are weighted by the occurrence frequency of each result.

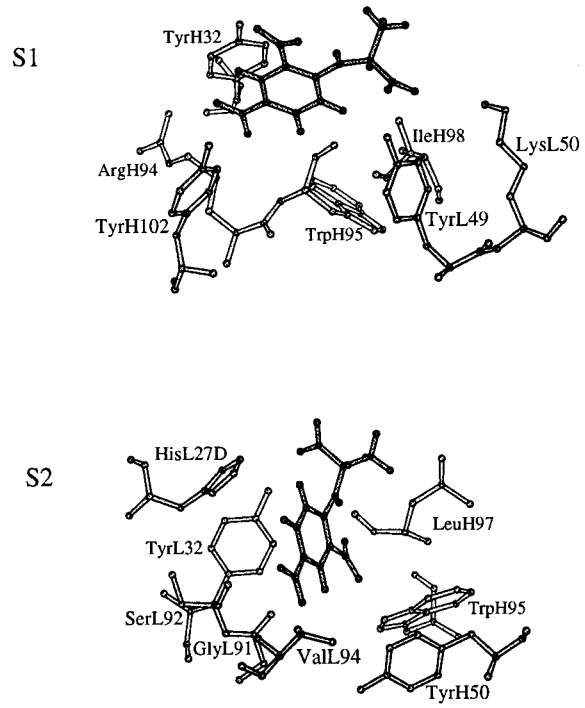

FIGURE 5 Architecture of the Lb4 subsites S1 (*top*) and S2 (*bottom*) with DNP-Ala as bound ligand, showing the DNP-Ala docking results and contact residues listed in Table 4.

Measuring the distances between geometric subsite centers and geometric centers of the ligands provides a useful overview of the location of the results. The residues mentioned above (which are also listed in Table 4) were used to define the subsite centers. With this definition, the S1 center turns out to be 9.0 Å from the S2 center. Structures accommodated within one of the subsites show, in general, distances to the subsite centers of 2.9–5.9 Å. Average values for all results are given in Table 3.

To summarize the data, the docking procedure has reproposed the binding site (S2) found in previous work (Sotriffer et al., 1996; Winger et al., 1996). In addition, it has revealed a new site within the CDRs (S1), where favorable interactions are possible. According to the docking energies, binding to S1 should even be more favorable than binding to S2. Docking positions outside these two sites are not taken into further consideration. Although some members of this set show good docking energies and occur with high frequency (especially in the case of DNP-Ala), they are classified as artifacts and false positives because of their location outside the CDRs or because of their "superficial" sticking to the surface.

Starting configurations for subsequent free energy simulations were thus selected from S1 and S2 results. The chosen results are presented in detail in Table 4. The selection was based primarily on the similarity with results of the other ligands. As described in Materials and Methods section, simulations were started from DNP-Ala and DNP-Ser; therefore no DNP-Gly complex structure was required as starting point. Nevertheless, it had to be ensured that DNP-Gly shows the same binding mode as the other two ligands.

In both subsites highly overlapping results were found for all three ligands. Consequently, simulations were started for both types of complexes (S1 and S2) to strengthen support for one or the other of the two subsites as the primary binding site. To analyze the similarity of the binding positions, the atoms of the conserved DNP part were used to measure the rmsd between the three molecules. Very low values were obtained for DNP-Ala and DNP-Gly, which bind almost identically in both subsites (rmsd of 0.98 Å in S1 and 0.33 Å in S2). As expected from the more different side chain of DNP-Ser, the fit is not as close for DNP-Ala and DNP-Ser (1.94 Å in S1 and 3.94 Å in S2) or DNP-Gly and DNP-Ser (2.52 Å in S1 and 3.95 Å in S2). In S1 the difference in DNP-Ser arises from a somewhat larger distance to Tyr H102, which is probably due to a hydrogen bond of the hydroxyl group with Lys L50. In S2 the aromatic part of DNP-Ser lies in the same plane as the aromatic rings of DNP-Ala and DNP-Gly, but with different orientations of the nitro groups and with closer contact to Gly L91 instead of Val L94 and His L27D. Despite these variations, the positions obtained for DNP-Ser can serve as starting point for free energy simulations and mutations toward DNP-Ala and DNP-Gly, as all results have been obtained by docking to a rigid antibody, and the inclusion of full flexibility may level off these differences.

TABLE 4 Docking results selected for investigation by free energy simulations (energies in kcal/mol)

	DNP-Ala	DNP-Gly	DNP-Ser
Subsite 1			
Energy	−25.68	−24.48	−21.10
Total occurrence frequency	17	1	1
No. of contacts with			
Tyr H 32	20	21	19
Arg H 94	2	5	—
Trp H 95	7	8	5
Gly H 96	—	2	6
Ile H 98	15	18	19
Tyr H 102	14	19	3
Tyr L 49	7	8	8
Lys L 50	2	1	7
Subsite 2			
Energy	−24.45	−24.22	−19.94
Total occurrence frequency	4	4	3
No. of contacts with:			
Tyr H 50	—	—	9
Trp H 95	4	3	8
Leu H 97	23	9	8
His L 27D	14	14	7
Tyr L 32	5	11	10
Gly L 91	2	3	11
Ser L 92	5	6	—
Val L 94	14	14	1

Contact residues are shown only if at least one of the ligands has at least five contacts with the residue. Atomic van der Waals contacts are defined as described by Sheriff et al. (1987).

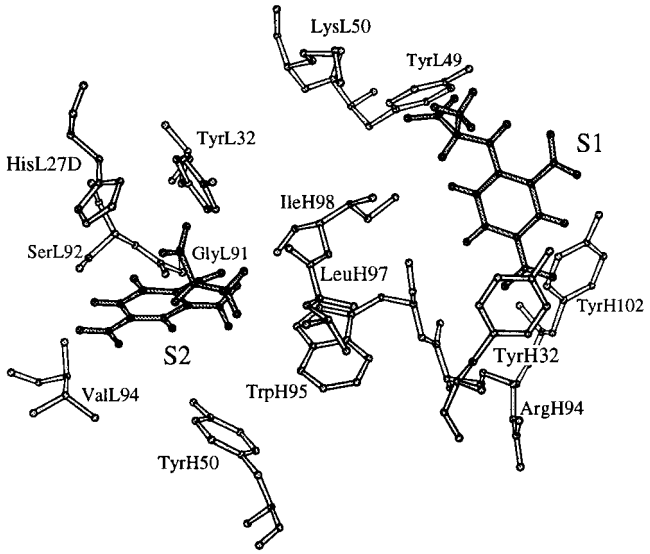

FIGURE 6 The complete Lb4 binding site with DNP-Ala as bound ligand, displayed simultaneously in S1 (*right*) and S2 (*left*), showing the DNP-Ala docking results and contact residues listed in Table 4.

Free energy calculations

Energetics

The perturbation of one ligand into the other in solution is the first step in calculations of relative free energies of

binding. The results of these simulations for the uncomplexed ligands are shown in the upper half of Table 5. The values given in the table are the averages of two runs in opposite directions (i.e., from $\lambda = 1$ to 0 and from 0 to 1). The hysteresis is the difference in the results for the forward and the backward run; half of its value is often taken as a crude error estimate (e.g., Fox et al., 1997). The last line of the first part shows the average over all eight simulation results (four simulations of different length, each done in both the forward and backward directions), with the standard deviation as an estimate of precision. In the last column the free energies of the three independent mutations are combined to a closed cycle, which serves as a measure of accuracy. It should be noted that the values presented here for the single transformations themselves have no straightforward physical meaning and cannot be compared to any experimental data, which is also partly due to the fact that all intra-perturbed group contributions were included in the calculations. Experimental observables arise only when the values are combined to yield relative free energy differences, as shown in Table 6.

The average free energy for the mutation of DNP-Ala to DNP-Gly in water is −27.4 kcal/mol, whereas mutating DNP-Ser into DNP-Ala is associated with a free energy change of +4.4 kcal/mol, and the perturbation of DNP-Ser into DNP-Gly gives a value of −23.0 kcal/mol. Taken together, these values lead to a perfect cycle closure energy of 0.0 kcal/mol, which is somewhat fortuitous and is probably associated with an uncertainty of 1 kcal/mol, as estimated from the combined standard deviations. The values of the single simulations improve in quality with longer simulation times, as indicated by smaller hystereses and cycle closure errors. The perturbations required for mutating DNP-Ala into DNP-Gly and DNP-Ser into DNP-Ala are rather simple. Already with short simulation times, fairly

TABLE 6 Relative free energies of binding calculated from the averages of the uncomplexed ligand runs and the results of the 4/4/168 complex runs, in comparison with experimental values

	A → G	S → A	S → G	Cycle Closure: A → G → S → A
Exptl. $\Delta\Delta G$	−0.7	+0.2	−0.5	0.0
S1 complexes				
ΔG complex	−28.89	+4.72	−24.30	+0.13
ΔG uncomplexed	−27.39	+4.44	−22.95	0.00
$\Delta\Delta G$	−1.50	+0.28	−1.35	+0.13
S2 complexes				
ΔG complex	−27.60	+3.30	−25.11	+0.81
ΔG uncomplexed	−27.39	+4.44	−22.95	0.00
$\Delta\Delta G$	−0.21	−1.14	−2.16	+0.81

All energies are given in kcal/mol. A, G, S stand for DNP-Ala, DNP-Gly, DNP-Ser, respectively. S1 and S2 refer to complexation at the two different subsites.

TABLE 5 Calculated free energies (in kcal/mol) A, G, S stand for DNP-Ala, DNP-Gly, DNP-Ser, respectively

Simulation Times eq/dc/total (ps)	A → G	S → A	S → G	Cycle Closure: A → G → S → A
Uncomplexed ligand in solution				
2/2/84	−27.37 (0.62)	+3.97 (0.45)	−22.79 (2.28) −20.45[e], −2.35	−0.61
4/4/168	−27.20 (1.49)	+4.94 (0.49)	−23.15 (0.93) −20.57[e], −2.59	+0.89
6/6/252	−27.49 (0.25)	+4.26 (0.35)	−22.72 (2.06) −20.38[e], −2.34	−0.51
10/10/420	−27.48 (0.17)	+4.61 (0.12)	−23.14 (0.09) −20.25[e], −2.89	+0.27
Average	−27.39	+4.44	−22.95	0.00
SD	0.43	0.41	0.83	(1.02)[†]
Complex: ligand in S1				
2/2/84	−28.22 (0.25)			
4/4/168	−28.89 (0.89)	+4.72 (0.48)	−24.30 (2.06) −21.06[e], −3.23	+0.13
10/10/420	−28.98 (0.50)			
Average	−28.70			
SD	0.46			
Complex: ligand in S2				
2/2/84	−25.67 (0.61)			
4/4/168	−27.60 (3.51)	+3.30 (0.41)	−25.11 (1.82) −21.65[e], −3.45	+0.81
10/10/420	−27.18 (0.83)			
Average	−26.81			
SD	1.34			

S1 and S2 refer to complexation at the two different subsites. Values in parentheses represent the hysteresis. For S → G, electrostatic decoupling was used. Therefore, in this column the lines following the composite result show the results of the decoupled runs, with [e] denoting the electrostatic part.
[†]Calculated as the root of the sum of the standard deviations squared.

precise values are obtained (standard deviations of ~0.4 kcal/mol for the overall averages). The perturbation of DNP-Ser to DNP-Gly is somewhat more demanding and requires the deletion of a larger fragment. This is reflected by the necessity to use electrostatic decoupling to reduce numerical problems and avoid instabilities in the simulations. However, the error associated with this transformation may still be significantly larger than for the other two mutations. The hysteresis shows generally larger values, and it is probably only by chance that it vanishes almost completely in the longest simulation. The average result, however, fits the values of the other two mutations very well and perfectly closes the cycle.

Relative free energies of binding require as a second step the calculation of mutational free energies of the ligands complexed to their receptor. The results for the perturbations of DNP-Ala, DNP-Gly, and DNP-Ser into each other when bound to Lb4 are shown in the lower half of Table 5. The simulations for both types of complexation (at S1 and S2) are presented. Because these simulations are computationally much more demanding, series of simulations with varying times of equilibration and data collection have been carried out for only one example (DNP-Ala to DNP-Gly).

In the case of DNP-Ala to DNP-Gly at S1, the standard deviation (0.46 kcal/mol) for the average result (−28.70 kcal/mol) of this set is the same size as for the uncomplexed DNP-Ala to DNP-Gly mutations, and essentially the same result is obtained for the 168-ps simulation as for the 420-ps simulation. Because of the similarity of the investigated systems, it might be expected that the average values obtained from forward and backward simulations of 168 ps could already be good estimates for results of longer simulations. Furthermore, the cycle closure error is again very low, with 0.13 kcal/mol for the S1 simulations.

The performance of the S2 simulations does not appear to be as good, with a higher cycle closure error of 0.81 kcal/mol and a very large hysteresis for the DNP-Ala to DNP-Gly mutation over 168 ps. The series with increasing simulation lengths does not provide as consistent results as the S1 simulation series, although the average 168-ps and 420-ps results are again comparable in size. Possible structural explanations for this behavior of the S2 simulations are given below. In comparison to S1 binding, the obtained free energies differ considerably for all three mutations of S2 complexes.

The combination of the results of the uncomplexed and the complexed simulations provides the relative free energies of binding, which can be compared with the experimental data, as shown in Table 6. For the mutations in solution the overall averages are used; for the complex mutations the results of the 168-ps simulations are used.

For the S1 complexes, the calculated $\Delta\Delta G$ values compare well with experiment. The slight preference of DNP-Ser over DNP-Ala by 0.2 kcal/mol is almost exactly reproduced. The preference for DNP-Gly over DNP-Ala and DNP-Ser is somewhat overestimated ($\Delta\Delta G$ for DNP-Ala to DNP-Gly: calculated −1.50 kcal/mol, experimental −0.7 kcal/mol; for DNP-Ser to DNP-Gly: calculated −1.35 kcal/mol, experimental −0.5 kcal/mol). The obtained ranking is correct, with DNP-Gly predicted to bind better than DNP-Ser and the latter better than DNP-Ala.

For binding to S2, the simulation results do not compare well with experiment, except for the DNP-Ala to DNP-Gly value (−0.21 kcal/mol calculated versus −0.7 kcal/mol experimental), which, however, is associated with the largest uncertainty of all $\Delta\Delta G$ values due to the large hysteresis of the complex simulation (see Table 5). DNP-Ala is incorrectly predicted to bind better than DNP-Ser, and the favoring of DNP-Gly over DNP-Ser is largely overestimated. Furthermore, the values are inconsistent among each other because of the cycle closure error propagated from the S2 complex simulations.

Structural analysis

A requirement for sensible results of free energy calculations by MD simulations is that the structures are stable along the trajectory. To analyze this, rms deviations of the C-α atoms have been calculated and are shown in Table 7. The values are averages over the entire trajectory, with the exception of the MD equilibration, of which only the last 20 ps has been used to calculate the average. For the MD equilibration, the reference structure is the starting structure (the original Lb4 model, with the ligand in the docked position). For the free energy simulations, the measurements refer to the average structure obtained from the last 20 ps of MD equilibration. The starting model obtained by homology modeling and docking would be a somewhat ambiguous reference structure. In fact, MD equilibration is expected to lead to some changes in the initial structure due to the inclusion of solvent and the full flexibility of the protein, which may result in optimized interactions with the ligand.

The average rms deviations from the starting structure are in the range of 1.5–2 Å for the four MD equilibrations, which are acceptable values, given the special nature of the starting structure. For the free energy perturbations, the rms deviations are generally around or below 1.7 Å, except for the backward simulations of the DNP-Ser to DNP-Gly mutations. The best performance is again observed for the DNP-Ala to DNP-Gly mutations. The increasing trend in the rms value observed for all simulations when continuing in the backward direction is still within acceptable boundaries, although it suggests some drift.

Besides the stability of the overall antibody structure, special attention is devoted to the binding site and the behavior of the ligand within it. This is true first of all for the phase of MD equilibration, which may be considered a kind of optimization of the initial model. Visual inspection of the final structures of the MD equilibration in comparison with the starting structures shows what changes have occurred. In the S1 complexes of Lb4 with DNP-Ala and DNP-Ser, the ligand is shifted toward Tyr H32 (and away from Tyr L49 and Lys L50) in such a way that the interac-

TABLE 7 Trajectory averages of rms deviations (in Å) observed in the complex simulations for the C-α atoms, the binding site residues, and the ligand

	DNP-Ala S1	DNP-Ala S2	DNP-Ser S1	DNP-Ser S2		
MD equilibration						
C-α	1.88	1.78	1.48	2.09		
b.s.	2.70	2.29	1.85	2.85		
Ligand	3.33	1.71	3.34	3.33		
	A → G S1	A → G S2	S → A S1	S → A S2	S → G S1	S → G S2
4/4/168 forward runs						
C-α	0.95	1.10	0.98	1.23	1.62	1.47
b.s.	1.10	1.04	1.16	1.51	1.26	1.71
Ligand	2.08	1.80	1.07	1.43	2.35	1.63
4/4/168 reverse runs						
C-α	1.30	1.36	1.62	1.74	2.42	1.90
b.s.	1.41	1.43	2.51	2.24	1.68	2.46
Ligand	1.75	3.17	2.50	1.66	3.90	4.10

A, G, S stand for DNP-Ala, DNP-Gly, DNP-Ser, respectively. S1 and S2 denote the two different subsites. Further explanations regarding details of the measurements are given in the text. b.s., binding site residues.

tion surface with this Tyr side chain is increased and the coplanar stacking of the aromatic rings is improved. Thereby the phenyl ring of the ligand is somewhat rotated around its central (pseudo C6) axis. As a consequence, both nitro groups are more deeply buried within the pocket. In contrast, the amino acid side chain is more solvent exposed, and the hydrogen bonds of the carboxylate with Tyr L49 and Lys L50 are replaced by hydrogen bonds with water molecules. The position of the ligand appears to be improved within the binding site, with a tighter fit reflected by an increased number of atomic contacts. Quite importantly, DNP-Ala and DNP-Ser assume almost identical binding orientations.

This is not the case for the S2 complexes with DNP-Ala and DNP-Ser, in which the initial slight differences between the docked structures become more pronounced during MD equilibration. For DNP-Ala the orientation of the nitro groups remains almost unchanged, with the *ortho* nitro pointing toward CDR H3 and the *para* nitro oriented toward CDR L3. The aromatic ring is somewhat tilted away from His L27D and is no longer pointing vertically into the pocket. Although the amino acid side chain is more solvent exposed, the carboxylate is now hydrogen-bonded with Asn L28. For DNP-Ser, in contrast, the carboxylate has become completely solvent exposed, whereas the hydroxyl is within hydrogen-bonding distance to Leu H97. The aromatic ring is even more tilted than in the case of DNP-Ala and now is in closer contact with CDR H3 residues. The nitro groups, finally, are not as deeply buried as those of DNP-Ala and do not show any good possibility for hydrogen bonds.

The described local changes are also reflected in the rmsd and distance measurements listed in Tables 7 and 8. For these analyses the most important contact residues of both subsites have been selected, based on the final simulation structures (not the docking structures). Compared to Table 4, this new list of contact residues also reflects some of the changes observed during equilibration and provides a better reference for the analyses of the free energy simulations. For S1 the binding site is defined by Tyr H27, Thr H28, Tyr H32, Arg H94–Phe H99, and Tyr H102, whereas S2 is formed by Tyr H52, Trp H95, Leu H97, Ile H98, His L27D, Tyr L32, Gly L91, Ser L92, and Val L94–Leu L96. The heavy atoms of these residues are used for rms fitting, as well as for evaluation of the subsite centers. For the ligands the atoms of the aromatic part (including the nitro groups and the amino nitrogen, a total of 16 atoms) are used for the measurements, because these belong to the conserved part of the molecule and are not subject to torsional flexibility, facilitating positional measurements and comparisons among the three molecules.

During MD equilibration of the S1 complexes, the side chains of the contact residues show somewhat larger adjustments than the overall C-α structure (2.70 Å and 1.85 Å).

TABLE 8 Trajectory averages of distances (in Å) measured in the complex simulations, in comparison with the starting values

	A complex	S complex	A → G	S → A	S → G
Distance from ligand center to subsite center					
S1 starting structure	5.25	5.88			
S1 MD equilibration	3.62	3.99			
S1 4/4/168 forward			4.18	4.13	4.55
S1 4/4/168 reverse			3.99	5.54	5.25
S2 starting structure	3.30	2.29			
S2 MD equilibration	2.91	3.12			
S2 4/4/168 forward			4.16	2.95	2.82
S2 4/4/168 reverse			5.53	2.57	5.42
Distance from ligand center to Tyr H32					
S1 starting structure	4.83	5.41			
S1 MD equilibration	4.09	3.69			
S1 4/4/168 forward			3.85	3.59	3.76
S1 4/4/168 reverse			3.70	3.84	3.81

A, G, S stand for DNP-Ala, DNP-Gly, DNP-Ser, respectively. S1 and S2 denote the two different subsites.

The rms shift for both DNP-Ala and DNP-Ser in S1 is ~3.3 Å. The direction of this movement is immediately visible from the distance measurements: the distance of the ligand to the subsite center decreases from over 5 Å to below 4 Å in both cases. This is accompanied by a closer contact with the side chain of Tyr H32 (the distances in the table are measured between the centers of the two aromatic rings). This residue, in fact, turns out to be the most important interaction partner. The "stacking" binding mode with Tyr H32 is strictly conserved throughout all S1 free energy simulations, as shown by average values between 3.6 and 3.9 Å. Variations in the orientation of the ligand as reflected by slightly varying rms values and S1 center distances are the consequences of rotations in the plane of the aromatic ring and concerted fluctuations of the Tyr-DNP pair.

For the S2 complexes such a clear and conserved binding mode is not observed. The ligands appear to be rather loosely bound and show considerable flexibility during the simulation. This is underlined by the comparatively large fluctuations in the measured rms deviations, which assume values of up to 1.05 Å (fluctuations are not shown in the tables). The differences in orientation between the ligands and their positional fluctuations during the simulations are also reflected by the distances to the subsite center, which vary between 2.6 and 5.5 Å.

Discussion of free energy calculations

The structural findings presented above lend further support to the significance of the S1 results and provide possible explanations of why the S2 free energy calculations are inconsistent with experimental binding energies. Apparently, S2 is not suited to accommodate the ligands as well as S1, a fact that has already been indicated by the less favorable docking energies in S2. The larger differences in binding orientations and the higher fluctuations within the S2 binding site suggest that merely weaker interactions are possible in S2 and that, in comparison, only binding in S1 may lead to the free energies observed experimentally. Based on the simulation results, S1 thus appears to be the optimal binding site of Lb4 for DNP ligands. Nevertheless, the S2 pocket should not completely be ruled out as a possible alternative site, given that because of larger fluctuations and differences in binding orientations in this site, the calculated free energies are expected to be associated with larger errors (in contrast, other sources of numerical errors, such as the removal or insertion of atoms, should affect both the S1 and the S2 calculations in a similar way).

The S1 binding mode also allows us to rationalize the experimental binding energies in their absolute and relative sizes. The small differences in binding energy between DNP-Ala, DNP-Gly, and DNP-Ser are consequences of the fact that the major interaction partner is the common DNP moiety, whereas the amino acid side chain is, to a large extent, solvent exposed. Therefore, the differences in binding energy primarily arise from varying solvation preferences, which are only slightly modulated by the protein environment. The low affinity of the binding interaction can be understood from the lack of a deep burial of the whole molecule within a binding pocket. In fact, the ligand is kept in its bound state by not much more than the "stacking" interaction with Tyr H32 and some weak hydrogen bonds to the nitro groups.

To obtain the results presented here for the complex systems, a total of 5.3 ns of simulation time was required (a further 7.8-ns total simulation time was necessary for the uncomplexed systems). Using periodic solvent boxes and fully solvated and unconstrained systems, this is at the limits of what is currently feasible. Nevertheless, this setup was used because it represents a better and less artificial choice for performing MD simulations than other, less expensive variants. Furthermore, it has two advantages in the context of free energy calculations. First, it does not lead to any artificial contributions that may arise from extended wall region boundary conditions (van Gunsteren and Mark, 1992) or probably even from constraints on the complex itself (Lee, 1992). Second, it makes it possible to invoke a certain error cancellation effect due to the identical treatment of both legs of the thermodynamic cycle, i.e., the mutation of the free ligand in solution and its transformation in the antibody complex (van Gunsteren, 1993).

Instead of performing only one very long simulation, we repartitioned the total time to obtain indications about the quality of the calculations. Series of simulations of varying length have been carried out: the results were stable within reasonable boundaries. On the other hand, the study was designed in such a way that a closed cycle could be formulated among the investigated systems, allowing for an extra check of the reliability of the results: very low cycle closure errors were obtained. Taken together, these results suggest the simulations to be of sufficient quality to permit useful insights into the binding properties of antibody Lb4.

CONCLUSIONS

The binding of DNP-Ala, DNP-Gly, and DNP-Ser to antibody IgE Lb4 has been analyzed. Microcalorimetric measurements found the free energy of binding to be in the range of −7.3 to −6.6 kcal/mol, with DNP-Gly binding best and DNP-Ala showing the weakest interaction. These experimental findings were analyzed and rationalized in structural terms by a "complete" modeling study. The starting point was an antibody structure obtained by homology modeling (Droupadi et al., 1994). Extensive docking searches were carried out to localize possible binding sites for the three ligands, whereby two subsites (S1 and S2) within the CDRs were identified as the most probable candidates for interaction. Free energy calculations were performed for complexation in both subsites. Given the special nature of the ligands, it was possible to form a closed cycle of transformations among them and thus to obtain an additional criterion for the reliability of the calculated free energy values. The cycle closure errors were, in general,

very low, suggesting sufficiently high consistency of the results.

The experimental free energy differences could be reproduced only for binding to S1. Structural analysis of the simulation trajectories showed the S1 complexes to be characterized by a uniform binding mode, whereas ligand binding in S2 exhibited considerable variability. Furthermore, the binding mode in S1 is consistent with the low affinity and the small differences in binding energy between the three ligands: the packing is tight on one side of the molecule only, and the conserved DNP part is the major interaction partner. In summary, S1 is expected to be the "real" binding site of these DNP-ligands.

One merit of the presented computational studies is that they were carried out in an ab initio fashion, without any detailed experimental structural information as input. The combination of different standard computational techniques proved to be a valid approach for obtaining structural insights, because experimental free energy differences could be reproduced with the resulting models of the complexes. Most encouraging for further investigations of protein-ligand interactions is the fact that even relatively low affinity complexation and differences in fine specificity can be analyzed with reasonable accuracy. Nevertheless, it is clear that because of various methodological limitations, the predictive nature of the results remains associated with some uncertainty. The predictions should therefore be tested in future by experimental structural determinations using x-ray crystallography or NMR techniques.

The authors thank Mag. Rudolf Winger for helpful discussions and technical assistance and Margaret Nutley for ITC technical assistance.

This work was supported by grant P10229-MED from the Austrian Science Foundation. The Biological Microcalorimetry Facility in Glasgow (AC) is supported by the UK Biotechnology and Biological Sciences Research Council (BBSRC) and the Engineering and Physical Sciences Research Council (EPSRC).

REFERENCES

Arevalo, J. H., M. J. Taussig, and I. A. Wilson. 1993. Molecular basis of cross-reactivity and the limits of antibody-antigen complementarity. *Nature.* 365:859–863.

Bayly, C. I., P. Cieplak, W. D. Cornell, and P. A. Kollman. 1993. A well-behaved electrostatic potential based method using charge restraints for deriving atomic charges: the RESP model. *J. Phys. Chem.* 97:10269–10280.

Berendsen, H. J. C., J. P. M. Postma, W. F. van Gunsteren, A. Di Nola, and J. R. Haak. 1984. Molecular dynamics with coupling to an external bath. *J. Chem. Phys.* 81:3684–3690.

Beutler, T. C., A. E. Mark, R. C. van Schaik, P. R. Gerber, and W. F. van Gunsteren. 1994. Avoiding singularities and numerical instabilities in free energy calculations based on molecular simulations. *Chem. Phys. Lett.* 222:529–539.

Beveridge, D. L., and F. M. DiCapua. 1989. Free energy via molecular simulation: applications to chemical and biomolecular systems. *Annu. Rev. Biophys. Biophys. Chem.* 18:431–492.

Brünger, A. T., D. J. Leahy, T. R. Hynes, and R. O. Fox. 1991. 2.9 Å resolution structure of an anti-dinitrophenyl-spin-label monoclonal antibody Fab fragment with bound hapten. *J. Mol. Biol.* 221:239–256.

Carlin, R. J., C. Kamps-Holtzapple, and L. H. Stanker. 1994. Characterization of monoclonal anti-furosemide antibodies and molecular modeling studies of cross-reactive compounds. *Mol. Immunol.* 31:153–164.

Chappey, O., M. Debray, E. Niel, and J. M. Scherrmann. 1994. Association constants of monoclonal antibodies for hapten: heterogeneity of frequency distribution and possible relationship with hapten molecular weight. *J. Immunol. Methods.* 172:219–225.

Chitarra, V., P. M. Alzari, G. A. Bentley, T. N. Bhat, J.-L. Eiselé, A. Houdusse, J. Lescar, H. Souchon, and R. J. Poljak. 1993. Three-dimensional structure of a heteroclitic antigen-antibody cross-reaction complex. *Proc. Natl. Acad. Sci. USA.* 90:7711–7715.

Chothia, C., and A. M. Lesk. 1987. Canonical structures for the hypervariable regions of immunoglobulins. *J. Mol. Biol.* 196:901–917.

Cooper, A., and C. M. Johnson. 1994. Isothermal titration microcalorimetry. *In* Microscopy, Optical Spectroscopy, and Macroscopic Techniques. *Methods Mol. Biol.* 22:137–150.

Cornell, W. D., P. Cieplak, C. I. Bayly, I. R. Gould, K. M. Merz, Jr., D. M. Ferguson, D. C. Spellmeyer, T. Fox, J. W. Caldwell, and P. A. Kollman. 1995. A second generation force field for the simulation of proteins, nucleic acids, and organic molecules. *J. Am. Chem. Soc.* 117: 5179–5197.

Cornell, W. D., P. Cieplak, C. I. Bayly, and P. A. Kollman. 1993. Application of RESP charges to calculate conformational energies, hydrogen bond energies, and free energies of solvation. *J. Am. Chem. Soc.* 115: 9620–9631.

Coutinho, P. M., M. K. Dowd, and P. J. Reilly. 1997. Automated docking of monosaccharide substrates and analogues and methyl α-acarviosinide in the glucoamylase active site. *Proteins.* 27:235–248.

Czaja, M., F. F. Richards, and J. M. Varga. 1976. Polyfunctional antibodies. Their biology and inheritance. *Ann. Immunol. (Paris).* 127C: 253–260.

Droupadi, P. R., J. M. Varga, and D. S. Linthicum. 1994. Mechanism of allergenic cross-reactions. IV. Evidence for participation of aromatic residues in the ligand binding site of two multi-specific IgE monoclonal antibodies. *Mol. Immunol.* 31:537–548.

Essex, J. W., D. L. Severance, J. Tirado-Rives, and W. L. Jorgensen. 1997. Monte Carlo simulations for proteins: binding affinities for trypsin-benzamidine complexes via free-energy perturbations. *J. Phys. Chem. B.* 101:9663–9669.

Fisher, H. F., and N. Singh. 1995. Calorimetric methods for interpreting protein-ligand interactions. *Methods Enzymol.* 259:194–221.

Fox, T., T. S. Scanlan, and P. A. Kollman. 1997. Ligand binding in the catalytic antibody 17E8. A free energy perturbation study. *J. Am. Chem. Soc.* 119:11571–11577.

Friedman, A. R., V. A. Roberts, and J. A. Tainer. 1994. Predicting molecular interactions and inducible complementarity: fragment docking of Fab-peptide complexes. *Proteins.* 20:15–24.

Frisch, M. J., G. W. Trucks, H. B. Schlegel, P. M. W. Gill, B. G. Johnson, M. A. Robb, J. R. Cheeseman, T. Keith, G. A. Petersson, J. A. Montgomery, K. Raghavachari, M. A. Al-Laham, V. G. Zakrzewski, J. V. Ortiz, J. B. Foresman, J. Cioslowski, B. B. Stefanov, A. Nanayakkara, M. Challacombe, C. Y. Peng, P. Y. Ayala, W. Chen, M. W. Wong, J. L. Andres, E. S. Replogle, R. Gomperts, R. L. Martin, D. J. Fox, J. S. Binkley, D. J. Defrees, J. Baker, J. P. Stewart, M. Head-Gordon, C. Gonzalez, and J. A. Pople. 1995. Gaussian 94. Gaussian, Pittsburgh, PA.

Furusawa, S., and Z. Ovary. 1988. Heteroclitic antibodies: differences in fine specificity between monoclonal antibodies directed against dinitrophenyl and trinitrophenyl hapten. *Int. Arch. Allergy Appl. Immunol.* 85:238–243.

Goodsell, D. S., H. Lauble, C. D. Stout, and A. J. Olson. 1993. Automated docking in crystallography: analysis of the substrates of aconitase. *Proteins.* 17:1–10.

Goodsell, D. S., and A. J. Olson. 1990. Automated docking of substrates to proteins by simulated annealing. *Proteins.* 8:195–202.

Helms, V., and R. C. Wade. 1997. Free energy of hydration from thermodynamic integration: comparison of molecular mechanics force fields and evaluation of calculation accuracy. *J. Comput. Chem.* 18:449–462.

Jorgensen, W. L., J. Chandrasekhar, J. D. Madura, R. W. Impey, and M. L. Klein. 1983. Comparison of simple potential functions for simulating liquid water. *J. Chem. Phys.* 79:926–935.

Kabat, E. A., T. T. Wu, H. M. Perry, K. S. Gottesman, and C. Foeller. 1991. Sequences of Proteins of Immunological Interest, 5th edition. National Institutes of Health, Bethesda, MD.

Kofler, H., I. Schnegg, S. Geley, A. Helmberg, J. M. Varga, and R. Kofler. 1992. Mechanism of allergic cross-reactions. III. cDNA cloning and variable-region sequence analysis of two IgE antibodies specific for trinitrophenyl. *Mol. Immunol.* 29:161–166.

Kollman, P. 1993. Free energy calculations: applications to chemical and biochemical phenomena. *Chem. Rev.* 93:2395–2417.

Kraulis, P. J. 1991. MOLSCRIPT: a program to produce both detailed and schematic plots of protein structures. *J. Appl. Crystallogr.* 24:946–950.

Lamminmäki, U., B. O. Villoutreix, P. Jauria, P. Saviranta, M. Vihinen, L. Nilsson, O. Teleman, and T. Lövgren. 1997. Structural analysis of an anti-estradiol antibody. *Mol. Immunol.* 34:1215–1226.

Lee, C. 1992. Calculating binding energies. *Curr. Opin. Struct. Biol.* 2:217–222.

Mark, A. E., S. P. van Helden, P. E. Smith, L. H. M. Janssen, and W. F. van Gunsteren. 1994. Convergence properties of free energy calculations: α-cyclodextrin complexes as a case study. *J. Am. Chem. Soc.* 116:6293–6302.

Mehler, E. L., and T. Solmajer. 1991. Electrostatic effects in proteins: comparison of dielectric and charge models. *Protein Eng.* 4:903–910.

Morris, G. M., D. S. Goodsell, R. Huey, and A. J. Olson. 1996. Distributed automated docking of flexible ligands to proteins: parallel applications of AutoDock 2.4. *J. Comput. Aided Mol. Des.* 10:293–304.

Padlan, E. A. 1994. Anatomy of the antibody molecule. *Mol. Immunol.* 31:169–217.

Padlan, E. A. 1996. X-ray crystallography of antibodies. *Adv. Protein Chem.* 49:57–133.

Pearlman, D. A. 1994. A comparison of alternative approaches to free energy calculations. *J. Phys. Chem.* 98:1487–1493.

Pearlman, D. A., D. A. Case, J. W. Caldwell, W. S. Ross, T. E. Cheatham, III, S. DeBolt, D. M. Ferguson, G. L. Seibel, and P. A. Kollman. 1995a. AMBER, a package of computer programs for applying molecular mechanics, normal mode analysis, molecular dynamics and free energy calculations to simulate the structural and energetic properties of molecules. *Comput. Phys. Commun.* 91:1–42.

Pearlman, D. A., D. A. Case, J. W. Caldwell, W. S. Ross, T. E. Cheatham, III, D. M. Ferguson, G. L. Seibel, U. C. Singh, P. K. Weiner, and P. A. Kollman. 1995b. AMBER 4.1. University of California, San Francisco.

Pearlman, D. A., and P. R. Connelly. 1995. Determination of the differential effects of hydrogen bonding and water release on the binding of FK506 to native and $Tyr^{82} \rightarrow Phe^{82}$ FKBP-12 proteins using free energy simulations. *J. Mol. Biol.* 248:696–717.

Pearlman, D. A., and P. A. Kollman. 1991. The overlooked bond-stretching contribution in free energy perturbation calculations. *J. Chem. Phys.* 94:4532–4545.

Reynolds, C. A., P. M. King, and W. G. Richards. 1992. Free energy calculations in molecular biophysics. *Mol. Phys.* 76:251–273.

Richards, F. F., W. H. Konigsberg, R. W. Rosenstein, and J. M. Varga. 1975. On the specificity of antibodies. *Science.* 187:130–137.

Roggenbuck, D., H. König, B. Niemann, G. Schoenherr, S. Jahn, and T. Porstmann. 1994. Real-time biospecific interaction analysis of a natural human polyreactive monoclonal IgM antibody and its Fab and scFv fragments with several antigens. *Scand. J. Immunol.* 40:64–70.

Ryckaert, J. P., G. Ciccotti, and H. J. C. Berendsen. 1977. Numerical integration of the cartesian equations of motion of a system with constraints: molecular dynamics of *n*-alkanes. *J. Comput. Phys.* 23: 327–341.

Sheriff, S., W. A. Hendrickson, and J. L. Smith. 1987. Structure of myohemerythrin in the azidomet state at 1.7/1.3 Å resolution. *J. Mol. Biol.* 197:273–296.

Shreder, K., A. Harriman, and B. L. Iverson. 1996. Molecular recognition of a monoclonal antibody (AC1106) cross-reactive for derivatives of $Ru(bpy)_3^{2+}$ and $Ru(phen)_3^{2+}$. *J. Am. Chem. Soc.* 118:3192–3201.

Simmerling, C., T. Fox, and P. A. Kollman. 1998. Use of locally enhanced sampling in free energy calculations: testing and application to the $\alpha \rightarrow \beta$ anomerization of glucose. *J. Am. Chem. Soc.* 120:5771–5782.

Sotriffer, C. A., W. Flader, R. H. Winger, B. M. Rode, K. R. Liedl, and J. M. Varga. 1999. Automated docking of ligands to antibodies: methods and applications. *Methods: A Companion to Methods Enzymol.* (in press).

Sotriffer, C. A., R. H. Winger, K. R. Liedl, B. M. Rode, and J. M. Varga. 1996. Comparative docking studies on ligand binding to the multispecific antibodies IgE-La2 and IgE-Lb4. *J. Comput. Aided Mol. Des.* 10:305–320.

Straatsma, T. P. 1996. Free energy by molecular simulation. *In* Reviews in Computational Chemistry, Vol. 9. K. B. Lipkowitz and D. B. Boyd, editors. Wiley-VCH, New York. 81–127.

Straatsma, T. P., and J. A. McCammon. 1992. Computational alchemy. *Annu. Rev. Phys. Chem.* 43:407–435.

van Gunsteren, W. F. 1993. Molecular dynamics studies of proteins. *Curr. Opin. Struct. Biol.* 3:277–281.

van Gunsteren, W. F., and A. E. Mark. 1992. On the interpretation of biochemical data by molecular dynamics computer simulation. *Eur. J. Biochem.* 204:947–961.

Varga, J. M., G. Kalchschmid, G. F. Klein, and P. Fritsch. 1991. Mechanism of allergic cross-reactions. I. Multispecific binding of ligands to a mouse monoclonal anti-DNP IgE antibody. *Mol. Immunol.* 28:641–654.

Varga, J. M., G. Kalchschmid, G. F. Klein, and P. Fritsch. 1991. Mechanism of allergic cross-reactions. II. Cross-stimulation, by chemically unrelated ligands, of rat basophilic leukemia cells sensitized with an anti-DNP IgE antibody. *Mol. Immunol.* 28:655–659.

Winger, R. H., K. R. Liedl, C. A. Sotriffer, A. M. Gamper, B. M. Rode, R. T. Kroemer, and J. M. Varga. 1996. Prediction of IgE(Lb4)-ligand complex structures by automated docking. *J. Mol. Recognit.* 9:239–246.

Wiseman, T., S. Williston, J. F. Brandts, and L. Lin. 1989. Rapid measurement of binding constants and heats of binding using a new titration calorimeter. *Anal. Biochem.* 179:131–137.

Zacharias, M., T. P. Straatsma, and J. A. McCammon. 1994. Separation-shifted scaling, a new scaling method for Lennard-Jones interactions in thermodynamic integration. *J. Chem. Phys.* 100:9025–9031.